Numerical Analysis of Sheet metal Drawing and Redrawing Process

Shasha Dou[1,2], Jiansheng Xia[2],

1 Nanjing University of Aeronautics & Astronautics, Nanjin, Jiangsu, 211106, China
2 Yancheng Institute of Technology, Yancheng, Jiangsu, 224051, China

Corresponding author is Jiansheng Xia

Abstract
A methodology of formulating an elasto-plastic finite model, which is based on the assumption of Prandtl-Reuss flow rule and Hill's yield criterion respectively, the Updated Lagrangian Formulation (ULF), the four degenerated shell element. An extended rmin rule are used to formulate the boundary condition. The friction phenomenon of slippage and viscosity at the boundary interface is based on increment of revision Coulomb rule. The simulation and experiments are carried out to study the Drawing and Redrawing deformation process by die structure and parameter. Both results after compensation were provided reference for designers and analysts.
Keywords: ELASTOPLASTIC, FINITE ELEMENT, SHEET METAL, DRAWING AND REDRAWING

1. Introduction

Metal forming simulation is a complicated research work. Because it is a high geometric nonlinearity problem. There are the large displacement, large rotation and large strain, which caused by the die shape effect. In the drawing process, when punch resistance and side resistance is too large, there will be rupture phenomenon of fracture, thinning, wrinkling. It need multi drawing to complete deep drawing on some products. It reduces the shrinkage of the flange through multi drawing, not exceed the bearing force, avoid rupture of sheet forming [1-3].

In the late 1960s, the finite element analysis method was applied in the field of metal forming. According to Von Mises yield criterion, Prandtl-Reuss equations, Love. A. E. H. [4] application shell theory, ignoring the effect of bending, proposed to Speherical, ellipsoid, cylindrical, conical shape, analysed stress and strain distribution. M. Merklein [5] proposed two methods direct redrawing and reverse redrawing, pointed out the product quality is relationship with the stretch ratio and the lower mould radius.

Farshid Dehghani [6] applicated Barlat-Lian Simulating law and yield large deformation elastoplastic finite element method to analyse the deep drawing forming, found earring is an inevitable phenomenon during the drawing forming process. Sousa [7] optimized design parameters of V and U bending with the finite element method and Genetic algorithm (GA), those parameters including: punch and die radius, punch displacement and plate force.

2. Methodology

2.1. Constitutive Equations

The element analysis constitutive relation can be written as the formula (1) and (2) follow [8-11].

$$\overset{\circ}{\sigma}_{ij} = C^{ep}_{ijmn}\dot{\varepsilon}_{mn} \tag{1}$$

$$C^{ep}_{ijmn} = C^{e}_{ijmn} - \frac{C^{e}_{ijkl}C^{e}_{uv}\frac{\partial f}{\partial \sigma_{kl}}\frac{\partial f}{\partial \sigma_{uv}}}{C^{e}_{kluv}\frac{\partial f}{\partial \sigma_{kl}}\frac{\partial f}{\partial \sigma_{uv}} + H'\frac{\sigma_{uv}\frac{\partial f}{\partial \sigma_{uv}}}{\bar{\sigma}}} \tag{2}$$

Where, $\overset{\circ}{\sigma}_{ij}$ is Jaumann differential of σ_{ij}, C^{ep}_{ijmn} is the elastic-plastic module, C^{e}_{ijmn} is Elastic module, f is the initial yield function, H' is the strain hardening rate,

$\bar{\sigma}$ is Von Mises yield function. the Matrix C_{ijmn}^{ep} can be expressed as the formula(3)(4)(5).

$$\left[C^{ep}\right]=\left[C^{e}\right]-\frac{1}{S}\begin{bmatrix} S_1^2 & S_1S_2 & S_1S_3 & S_1S_4 & S_1S_5 & S_1S_6 \\ & S_2^2 & S_2S_3 & S_2S_4 & S_2S_5 & S_2S_6 \\ & & S_3^2 & S_3S_4 & S_3S_5 & S_3S_6 \\ & & & S_4^2 & S_4S_5 & S_4S_5 \\ & & & & S_5^2 & S_5S_6 \\ symm & & & & & S_6^2 \end{bmatrix} \tag{3}$$

Where,

$$S=\frac{4}{9}\bar{\sigma}^2H'+S_1\sigma'_{xx}+S_2\sigma'_{yy}+S_3\sigma'_{zz} +2S_4\sigma'_{yz}+2S_5\sigma'_{zx}+2S_6\sigma'_{xy} \tag{4}$$

$$S_1=2G\sigma'_{xx},\ S_2=2G\sigma'_{yy}\ S_3=2G\sigma'_{zz} \tag{5}$$

$$S_4=2G\sigma'_{yz},\ S_5=2G\sigma'_{zx},\ S_6=2G\sigma'_{xy} \tag{6}$$

σ'_{ij} is deviator of σ_{ij}, G is the friction flow potential, $G=\sigma_1^2+\sigma_2^2$, $\left[C^{e}\right]$ is the formula in minimum strain, which can be expressed as the formula(7) follow[12]:

$$\left[C^{e}\right]=\frac{E}{1+\nu}\begin{bmatrix} \frac{1-\nu}{1-2\nu} & \frac{1-\nu}{1-2\nu} & \frac{1-\nu}{1-2\nu} & 0 & 0 & 0 \\ & \frac{1-\nu}{1-2\nu} & \frac{1-\nu}{1-2\nu} & 0 & 0 & 0 \\ & & \frac{1-\nu}{1-2\nu} & 0 & 0 & 0 \\ & & & \frac{1}{2} & 0 & 0 \\ & & & & \frac{1}{2} & 0 \\ symm & & & & & \frac{1}{2} \end{bmatrix} \tag{7}$$

E is modulus of elasticity, v is Poisson's ratio. If the material is homogeneous and isotropic, the elasto-plastic rate equation can be written as the formula (8):

$$\overset{\circ}{\sigma}_{ij}=\frac{E}{1+\nu}\left[\delta_{ik}\delta_{jl}+\frac{\nu}{1-2\nu}\delta_{ij}\delta_{kl}-\frac{3\alpha\left(\frac{E}{1+\nu}\right)\sigma'_{ij}\sigma'_{kl}}{2\bar{\sigma}^2\left(\frac{2}{3}H'+\frac{E}{1+\nu}\right)}\right]\dot{\varepsilon}_{kl} \tag{8}$$

When α=1, it is a plastic stage; when α=0, it is the elastic stage or unloading stage.

Equivalent stress and equivalent plastic strain relations can express by n-power law formula (9):

$$\dot{\sigma}=C\left(\varepsilon_0+\dot{\varepsilon}_p\right)^n \tag{9}$$

C is material constant, n is strain hardening index; $\dot{\sigma}$ is the equivalent stress, $\dot{\varepsilon}_p$ is the equivalent plastic strain, ε_0 is the initial strain.

2.2. Virtual Work Principle

It descripts the elastic-plastic deformation with the updated Lagrangian formulation ULF [12], the Virtual work principle formulation can be shown as the formula (10)

$$\int_{V^E}\left(\ddot{\sigma}_{ij}-e\sigma_{ik}\dot{\varepsilon}_{kj}\right)\delta\dot{\varepsilon}_{ij}dV+\int_{V^E}\sigma_{jk}L_{ik}\delta L_{ij}dV=\int_{S_f}\dot{f}\delta v_i dS \tag{10}$$

$\ddot{\sigma}_{ij}$ is the Cauchy stress tensor, $\dot{\varepsilon}_{kj}$ is the rate of stress tensor, $\dot{\varepsilon}_{ij}$ is the strain tensor, σ_{jk} is the rate of strain tensor, $\delta\dot{\varepsilon}_{ij}$ is the virtual strain tensor of the point, δL_{ij} is the virtual velocity gradient tensor of the point, δv_i is the velocity component, $\dot{f}$ is surface force component, L_{ij} is velocity gradient tensor, V is unit volume, S is unit surface area.

Finite element analysis: the structure is divided into many small units which called discrete entity. Based on Large deformation stress and stress rate relation, the finite deformation of update Lagrangian formulation, material constitution relationship, the velocity distribution of each unit is shown as the formula (11)(12)(13):

$$\{v\}=\leq[N]\{\dot{d}\} \tag{11}$$

$$\{\dot{\varepsilon}\}=\leq[B]\{\dot{d}\} \tag{12}$$

$$\{L\}=\leq[M]\{\dot{d}\} \tag{13}$$

Where, $\{v\}$ is velocity, $\{\varepsilon\}$ is strain rate, $\{\dot{d}\}$ is velocity gradient, $[N]$ is shape function, $\{\dot{d}\}$ is nodal velocity, $[B]$ is strain rate-velocity matrix, $[M]$ is velocity gradient-velocity matrix.

The principle of virtual work equation and the constitutive equation based on update Lagrangian are linear equation. The formula can be written by the form of incremental representation.

After finite element discretization, the large deformation rigid general equation is written as the formula (14).

$$[K]\{\Delta u\}=\{\Delta F\} \tag{14}$$

Here, differentials of $[K]$ and $\{\Delta F\}$ are expressed as the formula (15)(16).

$$[K]=\sum_{\langle E\rangle}\int_{V^e}[B]^T\left(\left[C^{ep}\right]-[Q]\right)[B]dV+\sum_{\langle E\rangle}\int_{V^e}[E]^T[Z][E]dV \tag{15}$$

$$\{\Delta F\}=\sum_{\langle E\rangle}\int_{S^E}[N]^T\{\dot{f}\}dS\Delta t \tag{16}$$

Where, $[K]$ is the overall elastoplastic stiffness matrix; $\{\Delta F\}$ is the nodal displacement increment; $\{\Delta u\}$ is the nodal forces incremental; [Q] and [Z] are stress correction matrix.

2.3. Friction Processing

There is friction in sheet forming process, so we need to pay attention to materials and tools of the interface conditions. When the material moves along the tool surface curve of the slide, the contact force can be expressed as the formula (17).

$$F=F_l l+F_n n \tag{17}$$

F_l is radial force and F_n is normal force, and differential equation of F can be expressed a8s the formula(18)

$$\dot{F}=\dot{F}_l l+F_l\dot{l}+\dot{F}_n n+F_n\dot{n} \tag{18}$$

Here, $\dot{l}$ and $\dot{n}$ are expressed as the formula (19) (20):

$$\dot{l}=-\Delta u_l^{rel}/R \tag{19}$$

$$\dot{n}=\Delta u_l^{rel}/R \tag{20}$$

Where, R is tool radius, Δu_l^{rel} is the local relative velocity between the tool and nodes. The relative speed of nodes can be expressed as the formula (21):

$$\Delta u_l^{rel}=\Delta u_l-\dot{u}_{tool}\sin\theta \tag{21}$$

Where, Δu_l is the contact tangent displacement increment of nodes, $\dot{u}_{tool}$ is the displacement increment of tooling, θ is the rotation angle.

Here, $\dot{F}$ is expressed as follow the formula (22):

$$\begin{aligned}\dot{F}=&\left(\dot{F}_l-F_n\Delta u_l/R+F_n\dot{u}_{tool}\sin\theta/R\right)\cdot l\\&+\left(\dot{F}_n-F_l\Delta u_l/R-F_l\dot{u}_{tool}\sin\theta/R\right)\cdot n\end{aligned} \tag{22}$$

Rigid matrix of the contact nodes is expressed the formula (23):

$$\begin{bmatrix}K & \cdots & \cdots\\ \cdots & K_{11}+F_n/R & K_{12}\\ \cdots & K_{21}+F_n/R & K_{22}\end{bmatrix}\cdot\begin{Bmatrix}\cdots\\ \Delta u_l\\ \Delta u_n\end{Bmatrix}=\begin{Bmatrix}\cdots\\ \dot{F}_l+F_n\dot{u}_{tool}\sin\theta/R\\ \dot{F}_l-F_l\dot{u}_{tool}\sin\theta/R\end{Bmatrix} \tag{23}$$

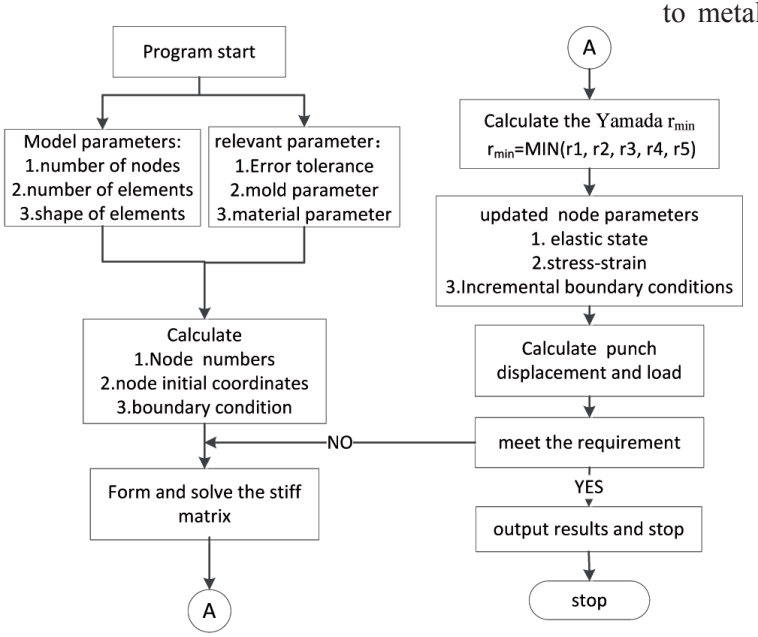

Figure 1. Simulation flow chart.

2.4. Numerical Analysis Flow

The 3d model design with the NX software, which is meshed with NASTRAN software follow. The whole analysis process is as shown in Fig. 1.

Based on the theory, the punch load, stress and strain, thickness are studied in the drawing and redrawing process. Simulation experiments were carried out with different parameters. Finally, the verification testings were carried out to verify the simulation, which can optimize and serve a reference for designer.

The model structures are composed of punch, die and blank holder, and as shown in Fig. 2.

There are two coordinates to solve the problem, one is the fixed coordinates (X, Y, Z), the other is the local coordinates (ξ, η, ζ). With the right-hand rule, the local coordinates (ξ, η, ζ) is used when nodes contact with the tool, and the fixed coordinates (X, Y, Z) is used when the nodes do not contact with the tool.

The structure of model is symmetrical, the 1/4 model is taken to finite element analysis.

The quadrilateral segmentation of degenerated shell element is used in sheet metal meshing, when four point quadrilateral degenerated shell element is used in the die meshing.

The part shape is round, the diameters is 82mm, 86mm and 90mm.

3. Results and Discussion

3.1. Load and displacement of the punch

Simulation analysis and experimental results are basically consistent. The relationship between load and displacement of one step drawing is that from the initial load to the maximum load, material sheet occurs flow deformation from punch to die. So it leads to metal processing hardening and the pressure in-

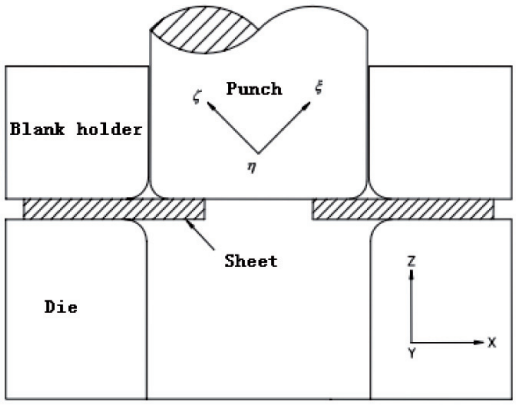

Figure 2. The sheet metal and die size chart.

creased significantly. The load increases slowly before the maximum load is reached. When the material sheet slides into the concave die, the load increases slowly to the maximum, because of the material sliding down and the middle concentration. When the sheet is divorced from the concave corner, there is only a one-dimensional channel, and the sheet contacts with the punch nose and die bottom wall. So the punch load decreases with stroke (as shown in Fig. 2).

In the second redrawing process, the part which formed by one step drawing is carried with the redrawing forming directly by the conical punch. With the increase of the material strength, the load increases obviously with the increase of stroke (as shown in Fig. 3).

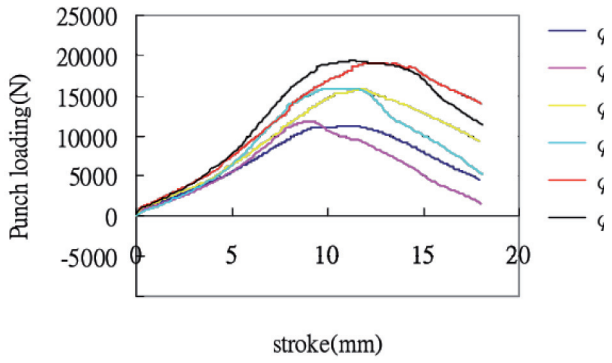

(a) one step drawing

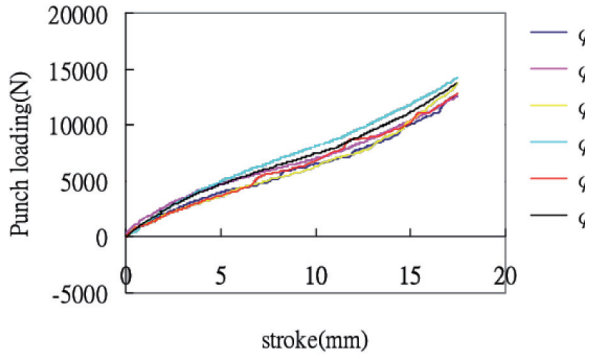

(b) Second step redrawing

Figure 3. Punch load and stroke diagram

3.2. Deformation history

One step drawing springback simulation chart is shown in Fig. (4)(a). The sheet is affected by the compression stress of the circumference in forming process, and there is a phenomenon of hardening. Two step redrawing springback simulation chart is shown in Fig. (4)(b), the shape of sheet turns from round cup to conical cup.

3.3. Stress Distribution Analysis

As can be seen from the result of simulation in Fig. (5), when the diameter is 86mm with different stroke. The one step drawing is as Fig. (5) (a), and the two steps drawing and redrawing is shown in Fig. (5) (b). The initial stress mainly concentrates in fillet of die and punch. When the stroke is from 8 to 19mm, the mainly stress concentrates in punch fillet, some stress slightly in bottom. But in the two steps drawing, the stress distribution is more uniform, no stress concentration, and better than one stage drawing.

3.4. Thickness Analysis

After drawing, there were different stress in Drawing and Redrawing process of the sheet mental. Thickness would be thinner. In order to study the change rules between the thickness and different drawing types, two simulation experiments were ar-

(a) One step drawing (b) Second step redrawing

Figure 4. Deformation history of sheet.

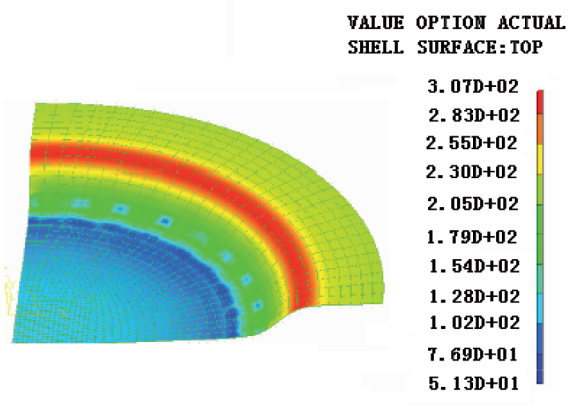

(a) One step drawing

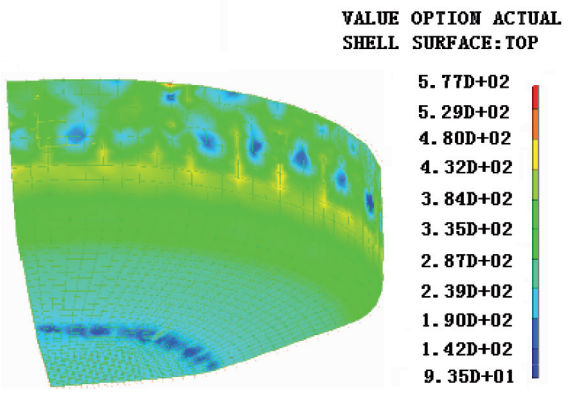

(b) Second step redrawing

Figure 5. Stress distribution chart

ranged. One is one stage drawing, the other is two stages drawing and redrawing. The simulation thickness results in different positions is shown in Fig. (6), and the experiment data is shown in Fig. (7). The position values were measured and recorded as shown in Table 1.

Table 1. The thickness in different relative position and different parameters

Position	Two steps drawing and redrawing(mm)			One step drawing(mm)		
	Sim	Exp	Error	Sim	Exp	Error
A	0.931	0.892	4.6%	0.892	0.870	2.5%
B	0.876	0.856	2.3%	0.841	0.827	1.6%
C	0.792	0.79	1. 5%	0.774	0.730	2%
D	0.697	0.71	0.6%	0.597	0.591	1.1%
E	0.744	0.74	0.4%	0.626	0.61	2.6%

* note: Sim is the simulation data; Exp is the experiment data.

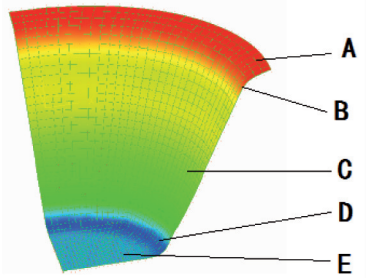

Figure 6. Measurement positions chart

(a) One step drawing (b) Two step drawing and redrawing

Figure 7. The experimental results drawing

Thickness distribution of sheet can be divided into three regions (as shown in Fig. 8). The relative positions are from the 0mm to 20mm; the sheet contacts to the punch closely; the thickness is no obvious change. The second area is from the 20mm to 40mm, the sheet is under the axial stress in the area of die fillet, and thin gradually. The third area is from the 40mm to 60mm, the sheet is squeezed into die accompany with punch movement; the sheet flow is hindered, and the thickness increases.

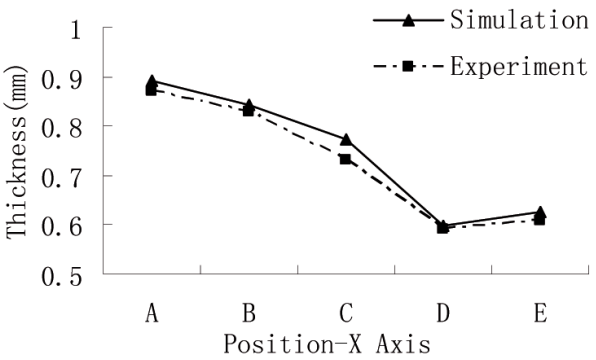

(a) One step drawing

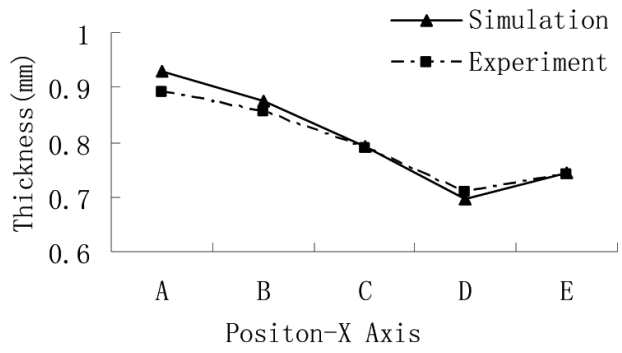

(b) second step redrawing

Figure 8. Thickness distribution

In the one step drawing, the sheet slides into die fillet by the influence of the friction, the material flow changes, occurred the thinning phenomenon, the thinnest point location is D, the value is 0.59mm, which is close to rupture (0.62mm). In the two steps drawing and redrawing, the average thickness about the same with the increasing of the punch stroke, and the minimum value D is 0.67mm.

Conclusions

Based on the numerical analysis and experimental results, combined with finite element method with the incremental elasto-plastic theory, analyzed warpage phenomenon in U-bending process of sheet metal, the following conclusions are obtained.

(1) During the drawing and redrawing deformation process, the stress and the thickness distribution of the figure in the experiment, the experimental value is quite close to the theoretical value.

(2) In one step drawing, the load is greater with the size of the sheet by the relationship between the punch and the load displacement, but the second step redrawing, the force roughly the same.

(3) Seen from the thickness distribution diagram, the thinnest position is in the corner of the punch and the material was extruded thickly in the end edge of piece. The second step redrawing is more thickness distribution.

Acknowledgements

This work was financially supported by The National Natural Science Foundation of China (No.51505408). The Natural Science Foundation for General Universities of Jiangsu Province, China (No.12KJD520010). The National Spark Program Project, China (No.2014GA690214). Jiangsu Intelligent Mould Manufacturing Engineering Technology Research Center.

References

1. Jiansheng Xia, Shasha Dou. Experimental Research on the Flanging Height Adjustment Based on Environmental Way International. Journal of Applied Environmental Sciences. 2013, 8(20), p.p. 2470-2489.
2. Jiansheng Xia, Shasha Dou. The study on steel elliptical cup drawing based on finite element analysis. Computer Modelling and New Technologies. 2014, 18(10), p.p. 7-13.
3. Jiansheng Xia, Shasha Dou. Numerical analysis of sheet metal U-Bending process. Computer Modelling and New Technologies. 2014, 18(11), p.p.159-165.
4. Love. A. E. H. A Ttreatise on The Mathematical Theory of Elasticity. Cambridge University Press, 2013,314 P.
5. M. Merkleina, J.M. Allwoodb, etc.. Bulk Forming of Sheet Metal. CIRP Annals - Manufacturing Technology. 2012, 61(2), p.p. 725-745.
6. Farshid Dehghani, Mahmoud Salimi. Analytical and Experimental Analysis of The Formability of Copper-stainless-steel 304L Clad Metal Sheets in Deep Drawing. The International Journal of Advanced Manufacturing Technology. 2015, 9, p.p.511-518.
7. L. C. Sousa, C. F. Castro and C. A. C. Antonio. Optimal Design of V and U Bending Processes Using Genetic Algorithms. Journal of Material Processing Technology. 2006,172, p.p.35-41.
8. S. Sezek, V. Savaz, B. Aksakal, Effect of die radius on blank holder force and drawing ratio: a model and experimental investigation, Mater. Manuf. Process. 2010, 25(7), p.p.557-564.
9. P.L. Menezes, S.V. Kailas, K.V. Kailas, Influence of die surface textures during metal forming a study using experiments and simulation. Mater. Manuf. Process. 2010, 25, p.p.1030–1039.
10. V. Vafaeesefat. Finite element simulation for blank shape optimization in sheet metal forming. Mater. Manuf. Process. 2011, 26, p.p.93-98.
11. J Xu, Z Tu, N Hu. Rotation Invariant Constitutive Relation for Reynolds Stress Structure Parameter. Applied Mathematics and Mechanics. 2015, 36(4), p.p. 517-522.
12. H. Laurenta, J. Coëra, b, P.Y. Manacha, M.C. Oliveirab, L.F. Menezesb. Experimental and Numerical Studies on The Warm Deep Drawing of An Al–Mg Alloy. International Journal of Mechanical Sciences. 2015, 93, p.p. 59-72.